Stability of nanocomposites of poly(ε-caprolactone) with tungsten trioxide

Ana V. Machado - Gabriela Botelho M. Manuela Silva - Isabel Correia Neves António M. Fonseca

Abstract

Nanocomposites of poly(ε-caprolactone) (PCL) and tungsten trioxide (WO_3) were prepared by solvent casting using 5 and 10% of WO_3 nanoparticles. The nanocomposites were characterized using several analytical techniques such as XRD, SEM, thermal analysis (TGA and DSC), spectroscopic methods (FTIR and UV/Vis) to gather information on the modifications introduced by WO_3. Photodegradation of PCL/WO_3 nanocomposites was studied exposing the samples to a Xenon lamp, which simulates the UV spectrum of the sun. The results obtained showed that due to the incorporation of WO_3 nanoparticles, the nanocomposites exhibit higher thermal stability together with higher photodegradation efficiency.

Keywords Nanocomposite · WO_3 · Poly(ε-caprolactone) · Photodegradation · Thermal stability

Introduction

Aliphatic polyesters such as poly(lactic acid) (PLA), poly (glycolic acid) (PGA), poly(ε-caprolactone) (PCL) and their copolymers are biodegradable polymers that have been

used in biomedical and industrial application due to their efficient biodegradability [1-3]. PCL is a linear, aliphatic thermoplastic, biocompatible, permeable, hydrophobic and biodegradable poly(ester), non-toxic for living organisms. PCL degrades slowly by hydrolysis of ester linkages, under suitable physiological conditions, over a fairly extended period. It is the most known biodegradable polymer used in a wide range of applications such as, packaging, medical devices, biodegradable suture and artificial skin [4-8]. Even though, this polymer exhibits attractive characteristics and properties, it has low tensile strength and low melting point [9, 10]. Moreover, it is semi-crystalline and the considerable crystallinity greatly inhibits its fast biodegradation [11].

Polymer degradation is influenced by several chemical and physical parameters such as molecular weight, amorphous phase content, moisture level, temperature and pH [5, 12]. Previous studies [13, 14] showed that the PCL photodegradability is higher than PLA, but not enough for some technological applications. This suggests that the chemical structure of the two sequential groups adjacent to the ester oxygen is crucial to determine the photodegradability of biodegradable polyesters. Many studies were made to develop new

polymeric materials using inorganic species, such as, titanium dioxide (TiO_2) in order to increase the photodegradability [15, 16]. The incorporation of some metal oxides into the polymeric matrix, can improve several properties of PCL, including its degradation rate. TiO_2 photocatalysis is known to generate reactive oxygenated species, i.e., $O^{-2}, HO_2^{\cdot}, HO^{\cdot}$, from H_2O or O_2 by oxidative or reductive reactions under UV. These chemical compounds increase degradation reactions, by attacking the polymer chain and promote successive chain cleavage [15, 16]. However, the films obtained do not present enough transparency for some

Fig. 1 Spectral energy distribution in wavelength 200 – 800 nm

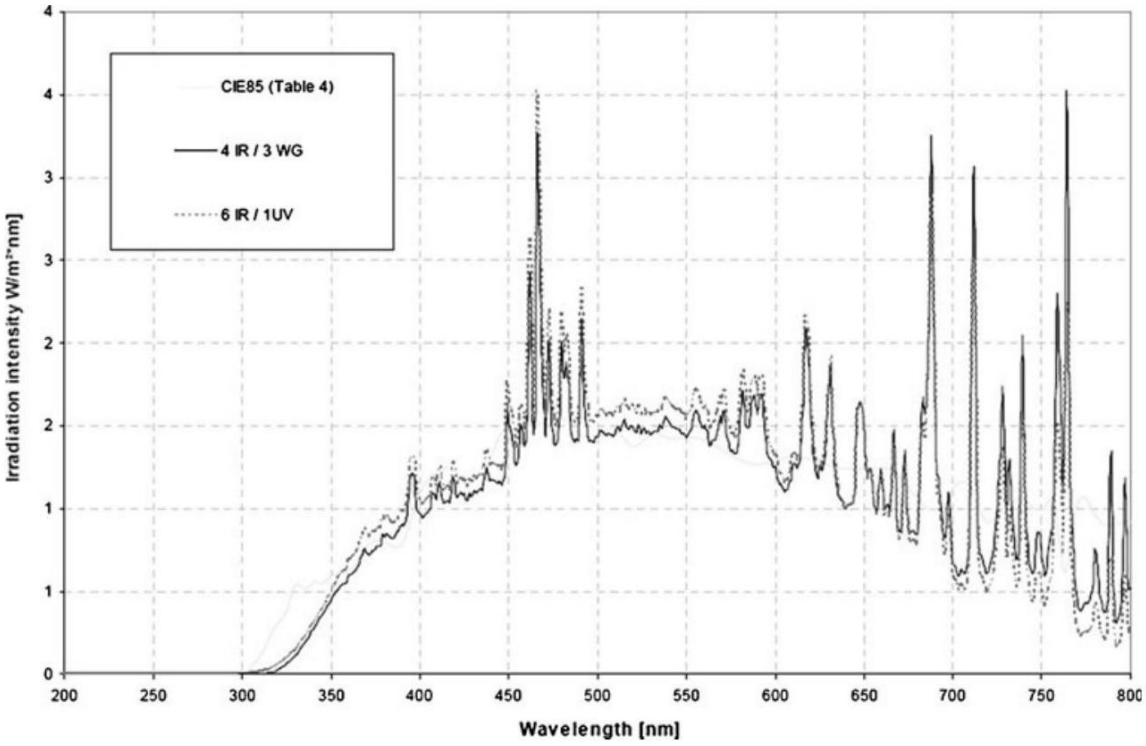

applications. To overcome this problem new organicinorganic nanocomposites were developed, using PCL as organic matrix and tungsten trioxide (WO_3) as inorganic specie. Tungsten trioxide was selected due to the photocatalytic properties [17]. Films were prepared by solvent cast, introducing different amounts of WO_3 nanoparticles by dispersion in the polymer matrix. Thermal analysis (TGA and DSC), surface analysis (XRD, SEM) and spectroscopic methods (FTIR and UV/Vis) were used to investigate and characterize the properties of the nanocomposite films as well as to study the influence of UV radiation on film properties.

The photodegradation of the prepared films was carried out in Xenon Test 150 S camera, under accelerated atmosphere conditions, such as, humidity and UV radiation. This degradation could be done displaying the films in natural environment, however this procedure takes too much time becoming impracticable the present investigation [18].

Experimental

Materials

Tungsten trioxide (WO_3) (99.75%, CAS: 1314-35-8) in powder form was purchased from British Drug House Chemicals Ltd (BDH) and toluene was analytical grade reagent from Aldrich and used without further purification. Poly(ε-caprolactone) (PCL) in granulated form, (Capa FB100, (MFI=0.4 g/10 min at 190 °C/2.16 kg), was kindly supplied by Solvay.

Preparation of PCL/WO_3 nanocomposites

The preparation of PCL/WO_3 nanocomposite films was performed according to the method developed by Nakayama [19]. Two samples were prepared using the same experimental conditions but different PCL/WO_3 weight ratio (5 and 10%). The highest amount used was 10% to assure mechanical performance and transparency. A representative preparation was as follows: PCL (2.0 g) was dissolved in 16 mL of Toluene. 5 and 10% (weight) of WO_3 in powder form was added to the PCL polymer solution prepared previously. Both solutions were mixed by stirring until they became homogeneous at room temperature. PCL film and the nanocomposite films with thickness around 40μ m were obtained by spreading the solution in a Teflon film. The solution was dried in Teflon film at room temperature during

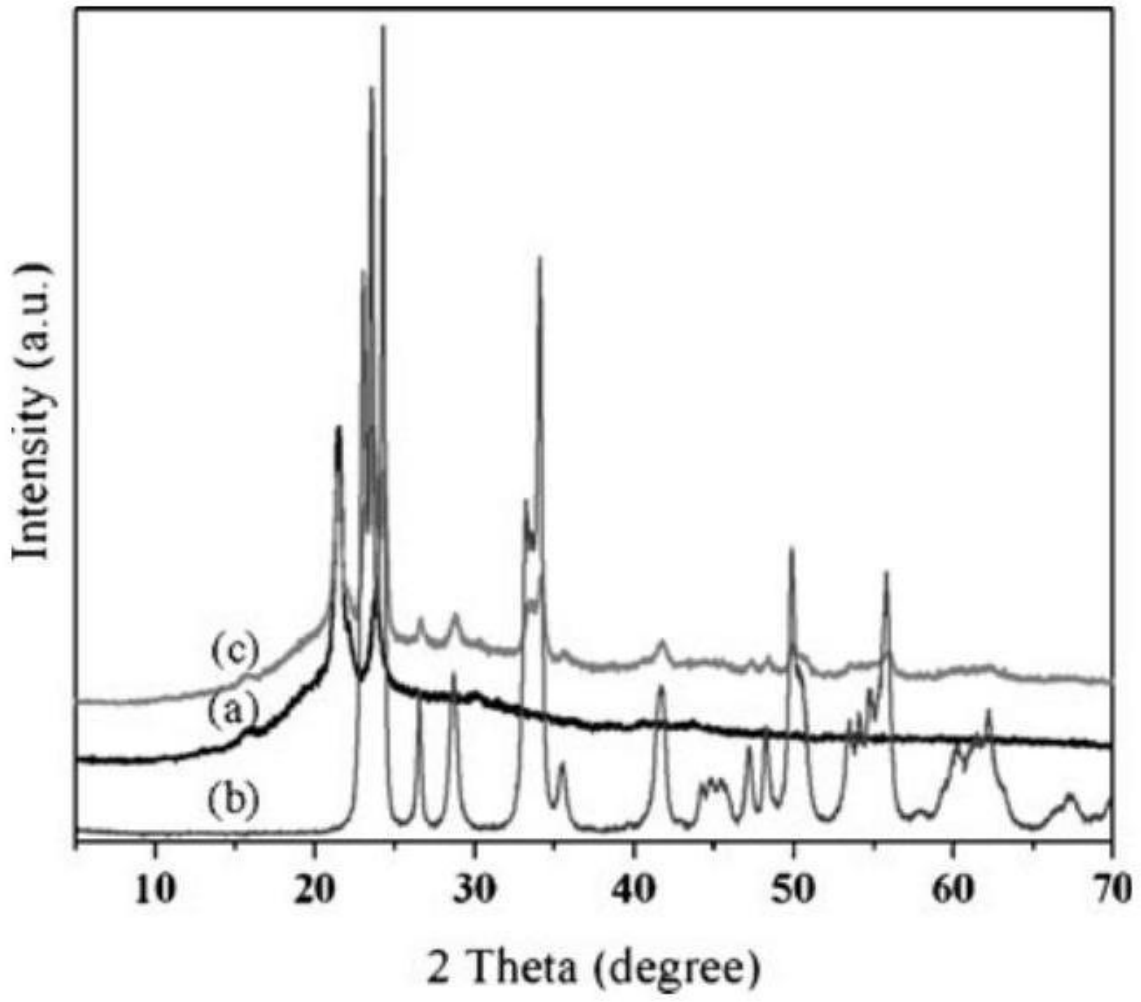

Fig. 2 XRD patterns of PCL (a), WO_3 (b) and PCL/ $WO_3 - 5$ (c)

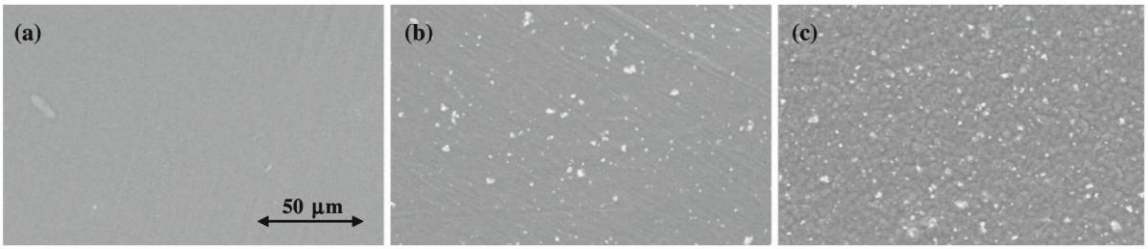

Fig. 3 SEM micrographs of PCL (a), PCL/ $WO_3 - 5$ (b) and PCL/ $WO_3 - 10$ (c) with the same resolution (× 500)

24 h. $PCL/WO_3 - x$ was defined as a film with x weight percent of WO_3, i.e., $PCL/WO_3 - 5$ and $PCL/WO_3 - 10$. The thickness of each film was measured with a pachymeter Mitutoyo with an accuracy of 0.010 mm .

Instrument and analytical procedures

Phase analysis was performed by XRD using a Philips PW1710 diffractometer. Scans were taken at room tempera-

Fig. 4 FTIR spectra of PCL, WO_3 and PCL/WO_3 – 5 a. in the range of $4000 - 500\ cm^{-1}$ and **b**. $900 - 600\ cm^{-1}$

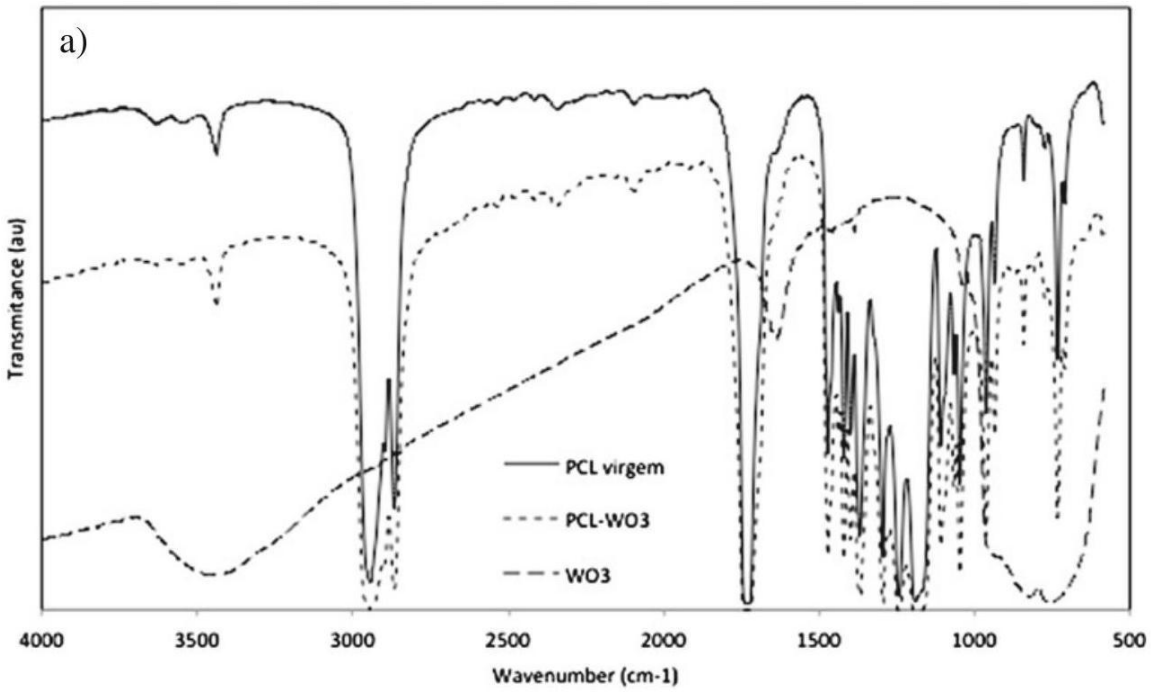

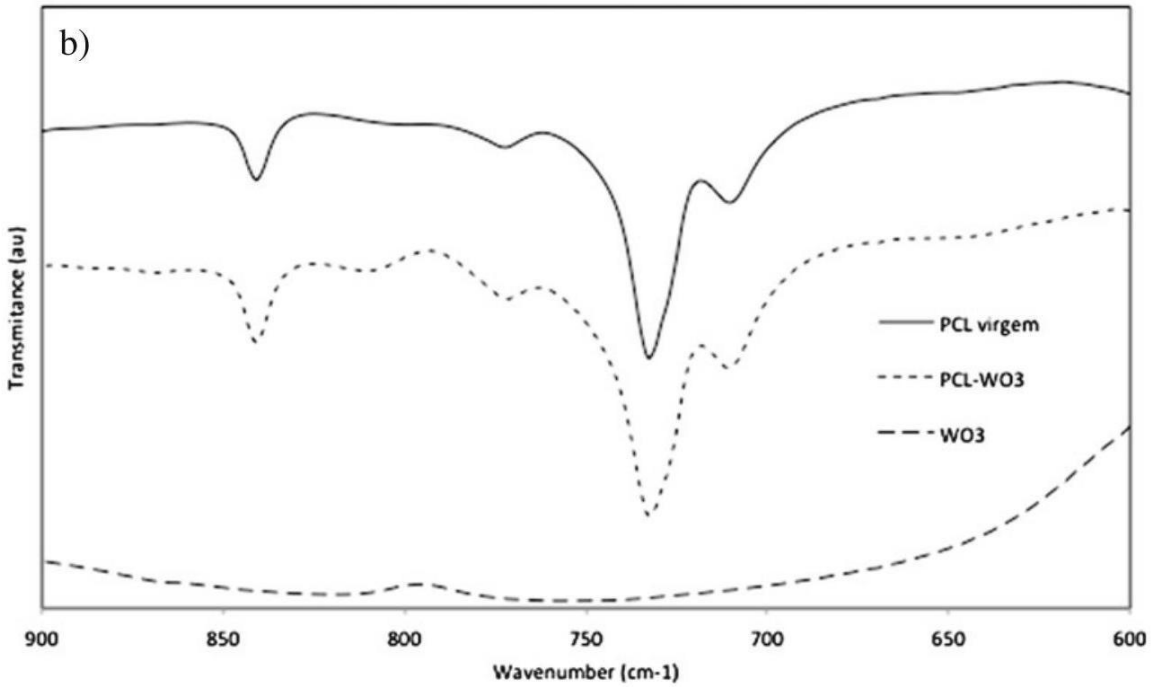

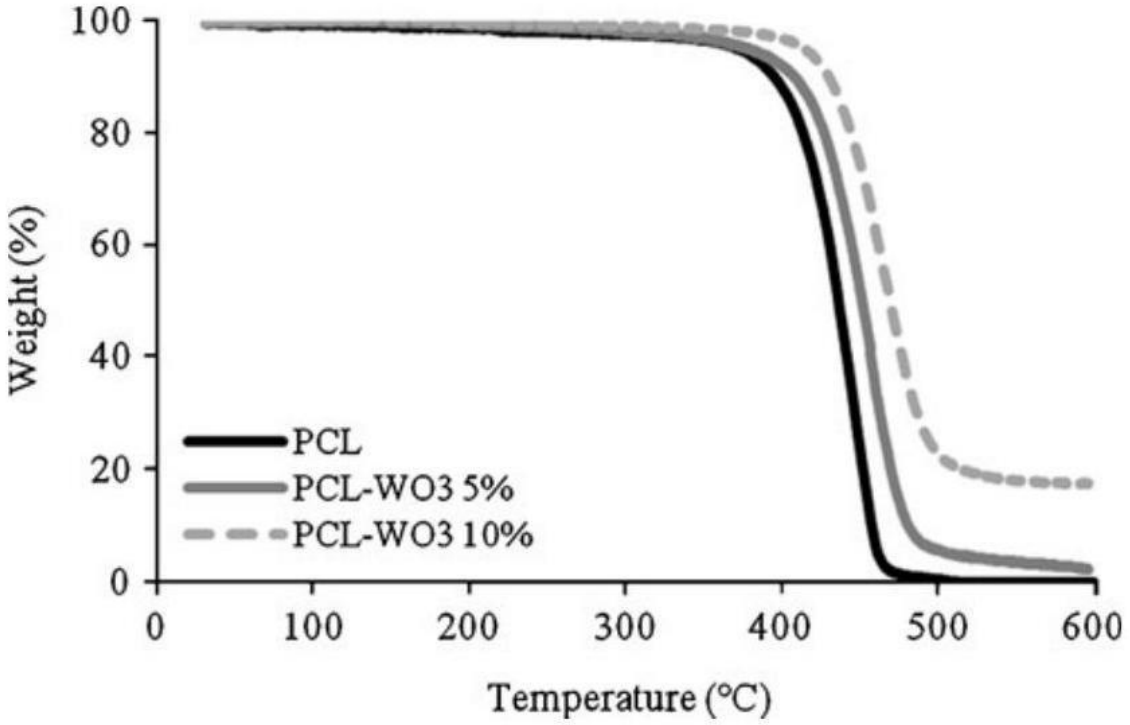

Fig. 5 Thermogravimetric curves of PCL and PCL/ WO_3 nanocomposites ture in a 2θ range between 4 and 70°, using $Cu - K\alpha$ radiation. The morphology of the nanocomposites was examined by scanning electron microcopy (SEM) using a LEICA Cambridge S360, which is equipped with an EDS system. To avoid the surface charging, prior to the analysis the samples were coated with gold in vacuum using a Fisons Instruments SC502 sputter coater. Room temperature Fourier Transform Infrared (FTIR) spectra of pure polymer (PCL) and of the nanocomposite films were measured using a FTLA 2000 spectrometer, in a range between 4000 and 500 cm^{-1} using 10 scans and a nominal resolution of 4 cm^{-1}. The samples were analysed as films in the case of PCL and nanocomposites, and KBr as pellets for WO_3. The electronic UV/Vis absorption spectra of samples were collected in the range of $700 - 200$ nm in a Shimadzu UV/2501PC spectrophotometer using a solid film support.

Thermal behaviour of the PCL and the nanocomposites ($PCL/WO_3 - 5$ and $PCL/WO_3 - 10$) nanocomposite films (before and after UV exposure) were investigated by thermogravimetry analysis (TGA) and differential scanning calorimetry (DSC). Samples for thermogravimetric studies were removed from dry films and transferred to open platinum crucibles and analyzed using a Rheometric Scientific TG 1000 thermobalance operating under a flowing argon atmosphere. A heating rate of 10 $°C min^{-1}$ was used and samples were heated from 30 to 600 °C, under argon atmosphere.

Differential scanning calorimetry measurements were performed using a Mettler DSC 821e, calibrated with

Table 1 Thermal properties of PCL and nanocomposites

Films	TGA T_{Onset} (°C)	DSC X_C (%)

PCL	409	40.9
PCL /WO_3 – 5	421	40.7
PCL /WO_3 – 10	438	40.5

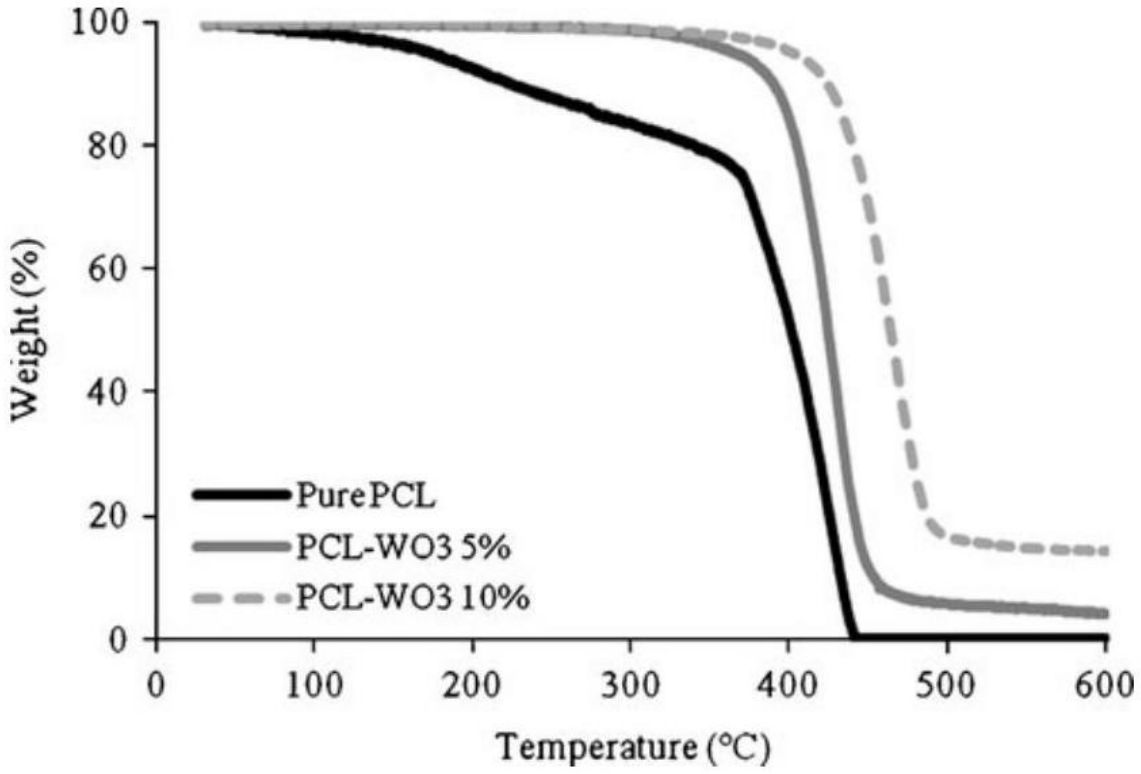

Fig. 6 Thermogravimetric curves of PCL and PCL/ WO_3 nanocomposites after 150 h UV exposure

indium to ensure the accuracy of the calorimetric scale. Samples were characterized in sealed 40μ L aluminum cans with perforated lids and subjected to thermal analysis under a flowing argon atmosphere (35 mL min^{-1}). In the preliminary phase of the study a variety of experimental conditions were applied to optimize heating rates for observation of the thermal events. Samples were heated from room temperature to 100°C at a rate of 5 °Cmin^{-1}. STARe software was used to evaluate the DSC curves. Degree of crystallinity (X_C) was calculated using the following equation [20]:

$$X_C = \frac{\Delta H_f}{\Delta H_f^0} \quad (1)$$

where ΔH_f is the apparent melt enthalpy (indicated in DSC curves as melting enthalpy per gram) corresponding to the component and ΔH_f^0 is the melt enthalpy per gram of the component in its completely crystalline state (139.5 J/g) [21].

Photodegradation of PCL/WO_3 nanocomposites

The photodegradation of films of PCL and nanocomposites, was carried out in a Xenotest 150*S* chamber from Heraeus (Original Hanau) equipped with a filtered Xenon lamp with

Table 2 Thermal properties of PCL and nanocomposites after 150 h of UV exposure

Films	TGA T_{Onset} (°C)	DSC X_C (%)
PCL	346	43.1
PCL /WO_3 – 5	399	50.6
PCL /WO_3 – 10	415	54.6

Fig. 7 Photodegradation of PCL via the Norrish II mechanism [13]

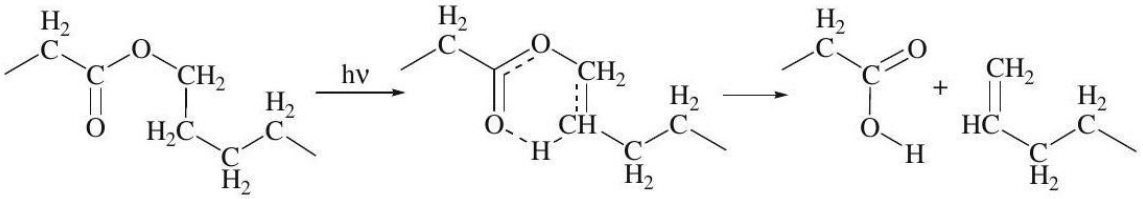

an intensity of 60Wm^{-2} according to standard procedures [22]. The light of the xenon lamp was filtered with a UV window combined with six IR filter glasses (according to Fig. 1). The samples were removed after 150 h of UV exposure and characterized by the analytical techniques indicated above.

Results and discussion

Characterization

The XRD diffraction patterns of PCL, nanocomposite films and WO_3 powder are shown in Fig. 2. Since the XRD diffractograms of nanocomposite films are very similar only the sample PCL/WO_3 – 5 is presented.

Both nanocomposites exhibited the typical and similar pattern of tungsten trioxide and PCL. As expected, the sharp peaks observed on PCL film diffractogram are typical of a crystalline material. The strong and sharp crystalline peaks at 21.5° and 23.9° are attributed to the [1 1 0] and [2 0 0] crystallographic plans of PCL crystal, respectively [23]. It is clear that the XRD patterns of the films are not severely affected by the introduction of the inorganic particles in the polymer structure and their crystallinity remains unaffected. In the PCL/ WO_3 – 5 film, the crystallinity indices of WO_3 nanoparticles did not change indicating the preservation of their structure.

Average crystal sizes of pure WO_3 nanoparticles and in nanocomposites films were estimated from the most intense reflection peak [1 0 1] by XRD line broadening using equation (2) known by the Scherrer equation, where D is the crystal size, K is a constant (0.9), λ the X-ray wavelength, B the peak with at a half-height and 2θ the position of the [h k l] reflection.

$$D = \frac{K\lambda}{B\cos\ \theta} \quad (2)$$

The [1 0 1] reflection for samples was fitted by a Gaussian profile to determine the peak widths at halfheight. The average crystal sizes of the pure WO_3 and those of nanocomposite films are similar, ranging between 6.3 and 6.7 nm.

The morphology of the nanocomposite films was evaluated by SEM. Figure 3 shows SEM micrographs of the PCL, PCL/ $WO_3 - 5$ and PCL/ $WO_3 - 10$.

The SEM micrographs show that the WO_3 nanoparticles are well dispersed in the PCL matrix. However, particles with different sizes can be noticed. For example, aggregates of WO_3 particles with a diameter of $3.1 - 12.5\mu$ m together with small particles with a diameter of $0.3 - 1.6\mu$ m.

FTIR analysis was performed to obtain information on the possible chemical interactions between PCL and WO_3. Figure 4 a and b depict the spectra of PCL, WO_3 and PCL/ $WO_3 - 5$ film in the range of $4000 - 500\ cm^{-1}$ and $900600\ cm^{-1}$, respectively.

The spectrum of PCL and nanocomposite films are dominated by strong polymer bands: two sharp bands at 2945 and $2866\ cm^{-1}$, which are attributed to the C-H symmetric stretching vibration of PCL, a strong band around $1730\ cm^{-1}$ is associated with carbonyl group of

Fig. 8 UV/Vis spectra PCL and PCL/ $WO_3 - 10\%$ before and after 150 h UV exposure

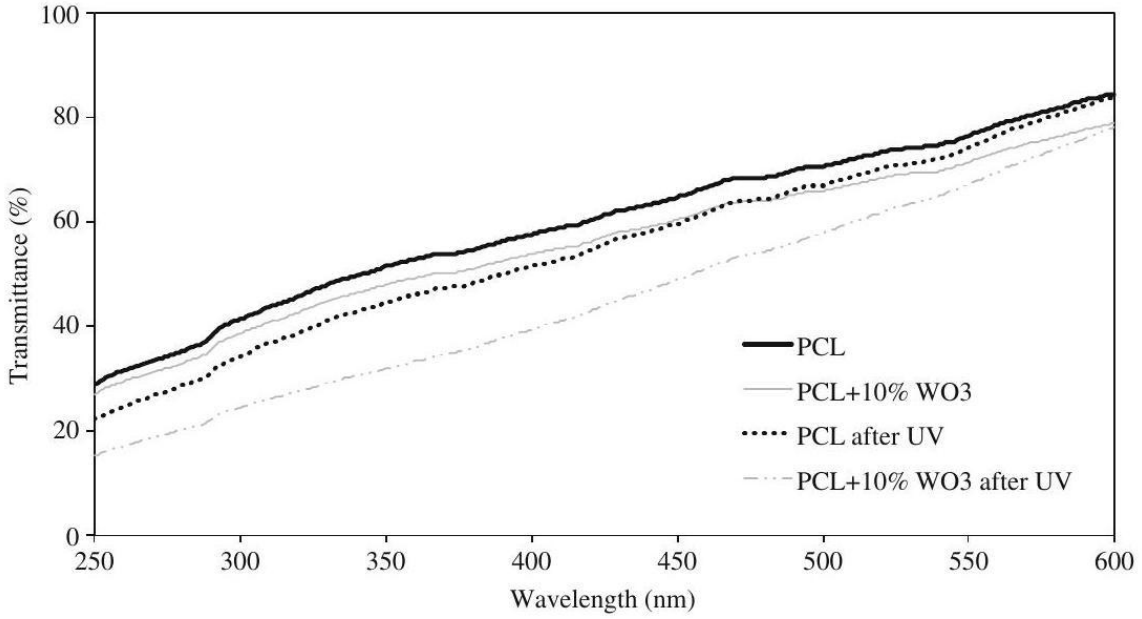

ester and the bands in the region of $1040 - 1500\ cm^{-1}$ are due to the vibration of $C - H, C - C$ and $C - O$ of PCL [23]. Figure 4a shows the typical spectrum of WO_3 nanoparticles where the characteristic band at $1637\ cm^{-1}$ is attributed to tungsten trioxide and the broad bands in the range $1000600\ cm^{-1}$ is ascribed to WO_3 vibration absorption. The FTIR

spectrum of nanocomposite film is similar to the one obtained for PCL, the only differences observed are in the range of 900-600 cm^{-1}. In Fig. 4b it can be clearly observed new bands at 870,814 and 648 cm^{-1}, which could be assigned to interactions between nanoparticles and polymer.

The thermal properties of PCL and prepared films were evaluated by TGA and DSC. The thermogravimetric analysis of the samples depicted in Fig. 5 show an apparent relationship between the onset temperature of the weight loss and the amount of WO_3 present in the films. The onset decomposition temperature (T_{Onset}), estimated by extrapolation from thermogravimetric curves is higher for the nanocomposites than for PCL. A summary of the results obtained from the thermogravimetric curves is shown in Table 1, where it can be observed that an acceptable thermal stability of about 409°C for the pure polymer increases about 3 and 7% for the $PCL/WO_3 - 5$ and $PCL/WO_3 - 10$, respectively. These results suggest that the incorporation of WO_3 improved the PCL thermal stability. Probably, these nanoparticles restrict the mobility of the polymer molecules, acting as thermal stabilizers [17, 24]. Similar behaviour was also observed by other authors with nafion and WO_3 nanoparticles [24].

The thermal stability results of the nanocomposites prepared evidence that they are adequate for application in a variety of technological devices.

To evaluate the effect of WO_3 nanoparticles on the crystallinity degree (X_c) of the films, DSC was performed and the results obtained are summarized in Table 1. The degree of crystallinity seems to be unaffected by the addition of WO_3 nanoparticles for both nanocomposites, being in agreement with the XRD results.

Photodegradability

The prepared nanocomposites and PCL films were exposed to UV radiation during 150 h . The influence of UV radiation on the nanocomposites thermal properties was assessed by TGA and DSC. The crystallinity degree and the onset decomposition temperature (Fig. 6) are presented in Table 2. The crystallinity increased from 40.7 to 50.6% for $PCL/WO_3 - 5$ and from 40.5 to 54.6% for $PCL/WO_3 - 10$. The increase of PCL crystallinity, in agreement with observations made by other authors [13, 25], can be explained by the thickening of crystallites. This can be associated with a decrease of the molecular weight. As it is known, PCL undergoes photodegradation by free radical process, which can lead to a breakdown of the polymer backbone via the

Norrish II mechanism at the ester group and the sequential two methylene groups adjacent to the ester oxygen as it can be seen in Fig. 7 [13, 26, 27]. Moreover, chain scission can also be enhanced by the presence of WO_3 due to it photocatalytic properties [17]. Thus, the increase of crystallinity of the nanocomposites can be associated with lower molecular size, which can orient more easily becoming more crystalline. Consequently the melting enthalpy increases with the UV radiation and WO_3 amount [28,29]. This proves unambiguously that WO_3 nanoparticles enhance the photodegradability of PCL.

By visual inspection, nanocomposite films ($PCL/WO_3 - 5$ and $PCL/WO_3 - 10$) showed slightly different appearance when compared to PCL film. The nanocomposites films transparency is lower due to the amount of WO_3 added.

Figure 8 shows the UV/Vis spectra of PCL and PCL/ WO_3-10 before and after UV exposure. While nanocomposite film exhibits higher transmittance decrease after irradiation, PCL film only changes slightly. The transmittance reduction till 400 nm implies that some UV absorbing chromophores, such as, oxygen containing functionalities and terminal double bonds were formed as a result of photodegradation, in agreement with the mechanism of Fig. 7. The results obtained evidence that WO_3 promotes PLC photodegradation.

Conclusions

In this work the influence of WO_3 nanoparticles on PCL film was investigated. From the results obtained it was concluded that WO_3 improves the photodegradability of PCL without losing its main properties. Moreover, this metal oxide not only enhances the polymer photodegradability but also increases the thermal stability, being both important characteristics for application of these materials in a variety of technological devices.

References

1. Holland SJ, Tighe BJ, Gould PLJ (1986) J Control Rel 4:155180
2. Kemnitzer JE, McCathy SP (1992) Macromolecules 25:59275934
3. Joseph DB (2000) The biomedical engineering handbook. CRC press
4. Ray SS, Okamoto M (2003) Macromol Rapid Comm 24:815840
5. Sahu LK, Britten K, Souza NA (2006) Proceedings of the Plastics Annual Technical Conference ANTEC. Charlotte, USA, pp. 1725-1730
6. Rak J, Ford JL, Rostron C, Walters V (2005) Pharm Acta Helv 60:162-169
7. Grijpma DW, Zondervan GJ, Penning AJ (1991) Polym Bull 25:327-227
8. Coombes AGA, Rizzi SC, Williamson M, Barralet JE, Downes S, Wallace WA (2004) Biomaterials 25:315-325
9. Pitt CG, Marks TA, Schindler A (1980) Controlled Release of Bioactive Materials. Academic Press
10. Tian D, Blacher S, Dubois P, Jerome (1998) Polymer 39:855-864
11. Li R, Nie K, Shen X, Wang S (2007) Mater Lett 61:1368-1371
12. Janik H, Justrebska M, Rutkawska M (1998) React Func Polym 38:27-30
13. Tsuji H, Echizen Y, Nishimura Y (2006) Polym Degrad Stab 91:1128-1137
14. Martins-Franchetti SM, Campos A, Egerton TA, White JR (2008) J Mater Sci 43:1063-1069
15. Cho S, Choi W (2001) J Photochem Photobiol A Chem 143:221228
16. Kim SH, Kwak S, Suzuki T (2006) Polymer 47:3005-3016
17. Zhang HJ, Chen GH, Bahnemann DW (2009) J Mater Chem 19:5089-5121
18. Duarte FM, Botelho G, Machado AV (2006) Polym Test 25:91-97
19. Nakayama N, Hayashi T (2007) Polym Degrad Stab 92:1255-1264

20. Turi EA (1981) In Thermal Characterization of Polymeric Materials. Academic, New York
21. Liu Q, Peng Z, Chen D (2007) Polym Eng Sci 47:460-466
22. ISO 4892-2 (2006) Plastics-Methods of exposure to laboratory light sources-Part 2: Xenon-arc lamps
23. Li R, Nie K, Shen X, Wang S (2007) Mater Lett 61:1368-1371
24. Yang J, Li Y, Huang Y, Liang J, Shen PK (2008) J Power Sources 177:56-60
25. Christensen PA, Egerton TA, Martins-Franchetti SM, Jin C, White J (2008) Polym Degrad Stab 93:305-309
26. Botelho G, Silva MM, Gonçalves AM, Sencadas V, Serrado-Nunes J, Lanceros-Mendez S (2008) Polym Test 27:818-822
27. Nieto-Gligorovski LI, Gligorovski S, Romanob R, Della Védovab C, Zetzscha C (2009) J Photochem Photobiol A Chem 204:46-51
28. Fornes TD, Paul DR (2003) Polymer 44:3945-3961
29. Leonard C, Halary JL, Monnerie L, Micheron F (1984) Polym Bull 11:195-202